

**CHAPTER 4**  
**SURFACE FREE ENERGY CHARACTERIZATION**  
**OF BASAL AND EDGE SURFACES OF TALC**  
**BY FLOW MICROCALORIMETRY**

**4.1. INTRODUCTION**

Talc is used for various applications, including paper coatings, pitch control, ceramics manufacture, and as filler in the plastics, polymer, paint and cosmetics industries. Particles of talc have the shape of platelets due to the layer structure of the mineral. It is well known that the basal surfaces are hydrophobic, while the edge surfaces are hydrophilic (1-2). The hydrophobicity of the basal surfaces arises from the fact that the atoms exposed on the surface are linked together by siloxane (Si-O-Si) bonds and, hence, do not form strong hydrogen bonds with water. The edge surfaces, on the other hand, are composed of hydroxyl ions, magnesium, silicon and substituted cations all of which undergo hydrolysis. As a result, the edges are hydrophilic, and they can form strong hydrogen bonds with water molecules and polar substances [3-5]. In many of the industrial applications, this dual surface property of the mineral plays an important role. In the paper industry, for the pitch and sticky control applications, the hydrophilic property of the edges allows the particles to be dispersed in aqueous media, while the hydrophobic property of the basal surfaces attract the sticky hydrophobic substances present in wood pulp.

For filler applications, proper control of the adhesion between talc filler and the matrix is essential in controlling the property of the composite material. The strength of adhesion depends on the surface properties of the filler and of the matrix (6). In general, strong filler-matrix interactions result in improved processability, impact strength, and surface quality, while interactions that are too weak lead to decreased strength and increased deformability of the composite (7). The role of acid-base interactions is crucially important in the use of minerals as filler.

It is well known that mineral fillers interact with polymers by acid-base interactions. For example, halogenated polymers such as polyvinylchloride are acidic and tend to interact strongly with basic fillers such as alumina and calcium carbonate (8). In this regard, if the

hydrophilic edge surface area of talc is appreciably higher, strong acid-base interactions between talc filler and polymer matrix would be expected. As a means of controlling the filler–polymer matrix interactions and improving the processability and properties of particulate filled polymers, talc filler is treated with appropriate surfactants (9, 10).

However, the talc ores from various deposits don't necessarily have unique physical, chemical, and mineralogical characteristics. Accordingly, the surface properties of the mineral vary with the geographical location of the mines, processing methods, particle size, surface treatment, etc. For example, there is a strong correlation defined between the surface hydrophobicity and particle size of talc, as reported in Chapter 2. The finer particles exhibited higher values of water contact angles and, hence lower values of total surface free energy ( $\gamma_s$ ) compared to those of larger particles. The increase in the surface hydrophobicity is attributed to the creation of more nonpolar basal plane surfaces upon grinding. It has to be mentioned that the surface free energy components reported in Chapter 2 and 3 are only the average of those at the basal and edge surfaces of talc.

Since the basal surface of talc is hydrophobic and the edge surface is hydrophilic, one can expect that the values of surface free energies ( $\gamma_s$ ) and its components ( $\gamma_s^{LW}$ ,  $\gamma_s^{AB}$ ,  $\gamma_s^-$  and  $\gamma_s^+$ ) at the basal surfaces should be different compared to those at the edge surfaces. However, until now, no attempts have been made to determine the surface free energy and its components at the basal and edge surfaces of talc individually. In fact, this is an extremely important subject, especially in the case of dealing with the minerals that have lamellar structure, e.g., talc, kaolin clay, graphite etc. Therefore, determination of surface properties both at the basal and edge surfaces of talc is essential for understanding the origin of molecular interaction and strength of adhesion between two interacting surfaces, i.e., talc and polymers, stickies, etc. It will also be helpful for the proper selection of surfactants used in the surface treatment of talc.

Flow microcalorimetry has been shown to be a powerful tool for characterizing solid surfaces and their interactions with liquids. Groszek used the flow microcalorimeter for the adsorption studies at liquid/solid interfaces (11, 12) and for determining the specific surface areas of solids (13). Templer (14) appears to have been the first to use the flow microcalorimeter for determining the heat of immersion enthalpies of various solid surfaces, namely ferric oxide, rutile and Graphon-81, in

different liquids. As discussed in Chapter 3, flow microcalorimeter can be used to estimate the contact angles of various liquids on talc powders as well. This is achieved by first measuring the heat of immersion enthalpies of talc samples in various liquids, and then, converting them into the contact angles using a rigorous thermodynamic relation.

Flow microcalorimetry can also be used to estimate the percentage of hydrophilic (polar) and hydrophobic (nonpolar) surface sites on powdered solid surfaces (15, 16). Groszek (15) developed a method of estimating the basal and edge surface areas of graphite and graphitized carbon blacks from flow microcalorimetric measurements. In this method, the hydrophobic surface percentages at the basal planes were estimated by the preferential adsorption of *n*-dotriacontane ( $nC_{32}$ ) from *n*-heptane (2 g/l) solution, whereas the hydrophilic surface area at the edge surfaces were determined by the preferential adsorption of butanol from *n*-heptane (2 g/l) solutions.

The acidity and basicity of powdered solid surfaces can also be determined using flow microcalorimetry. Basilio (17) conducted microcalorimetric measurements on chalcocite and pyrite surfaces to determine the differences in the surface acidity of these minerals. In this work, the heat of adsorption enthalpies of various organic bases from cyclohexane on chalcocite and pyrite were measured using a Microscal flow microcalorimeter. The heats of adsorption enthalpies were then used to estimate the values of the C and E parameters following Drago's acid-base interaction model. In Drago's model, the C and E parameters represent the softness and hardness of the solid surface, respectively. The experimental results showed that the surface acidity of pyrite is greater than the surface acidity of chalcocite, i.e., pyrite is a harder acid than chalcocite (17). Several other investigators have also used the flow type microcalorimeter to estimate the acidic and basic surface properties of powdered minerals and polymers (18, 19).

#### 4.1.1. Determination of Hydrophobic and Hydrophilic Surface Sites of Talc

Groszek and Partyka's (16) method may be used for estimating the hydrophobic and hydrophilic surface sites of talc samples. These authors suggested that instead of measuring the heats of wetting or adsorption of individual polar or apolar liquids, the measurement of heats of butanol adsorption from polar and apolar liquids on a solid

surface would permit a more accurate evaluation of relative hydrophobicity and would give more comparable results.

In this method, the heat of adsorption of butanol is measured from a butanol-in-water solution (10 g/l). The heat effect is mostly due to the adsorption of butanol on the hydrophobic sites of the sample, with the hydrocarbon tails in touch with the hydrophobic surface and the OH-groups pointing toward the aqueous phase, as schematically shown in Figure 4.1a. Thus, the heat effect is proportional to the hydrophobic surface area. By dividing this heat effect, given in units of mJ, with the heat of adsorption of butanol from water on graphon that is hydrophobic on all sites (17.6 mJ/m<sup>2</sup>), one can determine the hydrophobic surface area of the test solids.

One can also determine the area of the hydrophilic surface (i.e., edge surface) by contacting a talc sample with a butanol-in-n-heptane solution (2 g/l) using a flow microcalorimeter. The heat effect is largely due to the adsorption of butanol on the hydrophilic edge surface with the polar head (-OH groups) in touch with the surface and its hydrocarbon tails stretched in the n-heptane phase, as schematically shown in Figure 4.1b. Therefore, one can determine the percentage of hydrophilic surface by dividing the heat effect with the heat of adsorption of butanol on silica (197 mJ/m<sup>2</sup>) from n-heptane (20). Here, silica is chosen as a model reference solid, since it is hydrophilic on all sites, i.e., 100% hydrophilic. Thus, this method allows one to determine the hydrophobic and hydrophilic surface areas of unknown solids.

#### 4.1.2. Determination of Acidic and Basic Surface Sites of Talc

Fowkes et al. (6, 21-22) showed that when a solid is composed of acidic surface sites, it strongly interacts with basic sites of liquid probes. On the contrary, if the solid surface consists predominantly of basic sites, then these sites interact with acidic sites of liquid probes. Berg (23) explained the significant role of acid-base interactions between interacting liquid and solid surfaces by quantitatively determining the contribution from the acid-base interactions ( $W_a^{AB}$ ) to the overall work of adhesion,  $W_a$ .

The technique developed by Malhammar (19) can be used for estimating the acidic and basic surface sites of talc samples from flow microcalorimetric measurements. In this method, the number of basic sites of talc is determined by contacting the talc

surface with an organic acid (trifluoroacetic acid,  $pK_a=0.2$ ) from a 0.01 m/l toluene solution. The number of acidic surface sites is estimated from the adsorption of an organic base (butylamine,  $pK_a=10.77$ ) in toluene solution (0.01 m/l).

#### 4.1.3. Determination of Areal Ratios of Talc Samples

The shape and aspect ratios of particles have usually been evaluated by means of Transmission Electron Microscopy (TEM) and Scanning Electron Microscopy (SEM). Recently, sedimentation, light scattering, imaging and rheological measurement techniques have been used for measuring the particle size distribution and, hence, estimating the shape and aspect ratios of particles (24). However, these methods are time consuming and subjective, and only a few particles are analyzed to evaluate the properties of bulk particles. Obviously, more objective, rapid, and simple methods are required.

In the present work, a simple and very fast method is used for determining the basal surface area to edge surface area ratio (areal aspect ratio) values of talc particles. Essentially, the method of determining the values of the areal ratios of talc samples is the same as that of the estimation of the hydrophobic and hydrophilic surface area of talc samples, as described in Chapter 4.1.1. The areal ratio is then obtained from the ratio between the hydrophobic (basal) and hydrophilic (edge) surface area using the following relation:

$$\text{Areal aspect ratio} = \frac{\text{The area of basal (hydrophobic) surface}}{\text{The area of edge (hydrophilic) surface}} \quad [4.1]$$

In this method, the heat of adsorption ( $-\Delta H_{ads}$ ) of n-butanol on a talc sample is measured from a 2 g/l butanol-in-heptane solution. According to Malandrini, et al. (20), the n-butanol molecules adsorb on the edge surfaces of the talc particles with the hydroxyl groups in contact with the surface. By dividing the heat effect, given in mJ, with the heat of adsorption of butanol on silica ( $197 \text{ mJ/m}^2$ ), one obtains the area of the hydrophilic edge surface.

In another method, the heats of adsorption measurements are conducted in a 10 g/l butanol-in-water solution. The heat effect, which is due to the inverse orientation of n-

butanol in the basal surface, is divided by the heat of adsorption of butanol on graphon (17.6 mJ/m<sup>2</sup>) to obtain the area of the hydrophobic basal surface (16).

The summation of the hydrophobic and hydrophilic surface areas, determined in the manner described above, should give the total surface area of the talc sample under consideration. If the total surface area determined using this approach is in agreement with those obtained from the standard method, e.g. BET, one can confidently determine the ratio (or lamellarity) between the basal and edge surface areas.

The areal aspect ratio values obtained from the calorimetric heat of adsorption measurements are compared with those of dimensional aspect ratio values obtained using other techniques such as particle size measurement, etc.

#### 4.1.4. Surface Free Energy Characterization of Basal and Edge Surfaces

In order to determine the surface free energy components at the basal and edge surfaces of talc, surface free energy characterization studies must be conducted at two different sizes (at size  $x_1$  and  $x_2$ ). Each sample is subjected to surface free energy characterization studies as described in Chapter 2. The values of  $\gamma_s$ ,  $\gamma_s^{LW}$ ,  $\gamma_s^{AB}$ ,  $\gamma_s^+$ , and  $\gamma_s^-$  can be determined for each size ( $x_1$  and  $x_2$ ) using Eqs. [2.9] and [2.10].

From the basal to edge surface area ratios of the talc samples as determined using the procedure described in Chapter 4.1.3, the fraction of the basal surface ( $f_b^{x_1}$ ) and that of the edge surface ( $f_e^{x_1}$ ) at size  $x_1$  will be determined. One can then set up the following equation,

$$\gamma_s^{x_1} = f_b^{x_1} \gamma_s^b + f_e^{x_1} \gamma_s^e \quad [4.2]$$

in which  $\gamma_s^b$  is the total surface free energy ( $\gamma_s$ ) at the basal surface and  $\gamma_s^e$  is the same at the edge surface. Eq. [4.2] suggests that the value of  $\gamma_s$  determined using Eq. [2.10], is a composite of  $\gamma_s^b$  and  $\gamma_s^e$  in proportion to  $f_b^{x_1}$  and  $f_e^{x_1}$ . Similarly, one can set up the following equation at size  $x_2$ :

$$\gamma_S^{x_2} = f_b^{x_2} \gamma_S^b + f_e^{x_2} \gamma_S^e \quad [4.3]$$

An explicit assumption in writing Eqs. [4.2] and [4.3] is that  $\gamma_S^b$  and  $\gamma_S^e$  do not change with particle size, which is a reasonable assumption. Solving Eqs. [4.2] and [4.3] simultaneously, one can determine the values of  $\gamma_S^b$  and  $\gamma_S^e$ .

Likewise, one can set up simultaneous equations for  $\gamma_S^{LW}$ ,  $\gamma_S^{AB}$ ,  $\gamma_S^+$ , and  $\gamma_S^-$ , and obtain the respective values at the basal and edge surfaces of talc. To the best of our knowledge, this is completely new information and in the literature no such work has been done until now.

It was the primary objective of the present work to study the possibility of determining the surface free energies and their components at the basal and edge surfaces of powdered talc samples. In order to meet this objective, the contact angle values of a talc sample that is ground to two different sizes were determined using the thin layer wicking technique. In addition, the hydrophobic-hydrophilic surface area ratios of talc samples were obtained from flow microcalorimetric measurements. Thus, the surface free energy parameters at the basal and edge surfaces of talc could be estimated from the hydrophobic-hydrophilic surface fractions obtained and contact angles measured. This work also aimed to demonstrate the availability and importance of acid-base interactions between two interacting surfaces, e.g. liquid and solid surfaces from flow microcalorimetric measurements. It is obvious that the knowledge of surface free energy parameters both at the basal and edge surfaces of solid (e.g. talc) will be extremely useful for understanding the molecular origin of the adhesion between two interacting surfaces (e.g. talc and polymer).

## 4.2. EXPERIMENTAL

### 4.2.1. Materials

The experiments were carried out using various talc samples, which were obtained from the same sources as those stated in Chapters 2 and 3. The solvents used for these studies were HPLC (>99.5% purity) grade toluene and n-heptane from Aldrich

Chemical Company. They were dried overnight over 3 to 12 mesh Davidson 3-A molecular sieves before use. All the glassware was oven-dried for at least 24 hours at 75 °C prior to use. Solutions were prepared fresh daily before use in the experiments.

The organic acids and bases used in the microcalorimetric measurements were trifluoroacetic acid (HPLC grade from Sigma Chemicals) and butylamine (99.6% purity from Fisher Scientific). Butanol (HPLC grade) was purchased from Fluka and had a purity greater than 99.5%. The syringe, calorimeter cell, fittings and the teflon tubing lines of the microcalorimeter were cleaned using HPLC grade acetone (Fisher Scientific) after each run. All of the experiments were conducted at  $20 \pm 2$  °C.

#### 4.2.2. Experimental Apparatus and Procedure

Heats of adsorption measurements were conducted using a Model 3V flow microcalorimeter (FMC) from Microscal, United Kingdom. Figure 4.2 shows a schematic diagram of the calorimeter. The FMC has a teflon cell fitted in a metal block that is insulated with mineral wool. A calorimeter cell, made of teflon, was placed in a metal block, which was insulated from the ambient by mineral wool. Two glass-encapsulated thermistors were placed inside the cell to monitor the changes in temperature of the sample, and two reference thermistors were placed in the metal block outside the cell. These thermistors have sensitivity capable of detecting temperature changes as low as  $10^{-5}$  °C inside the cell. The calorimeter was calibrated by means of a calibration coil, which was placed in the sample bed. During the calibration, a known amount of electrical energy is passed through the coil in the sample bed while the solvent is being pumped through the bed. The entire unit was housed in a draft-proof enclosure to reduce the effect of temperature fluctuations in the ambient.

In each measurement, a talc sample was dried overnight in an oven at 110 °C. A known amount (usually 0.05-0.15 gram) of the dried sample was placed in the calorimeter cell, and degassed for at least 30 minutes under vacuum (<5 mbar) at ambient temperature. The vacuum system consisted of a vacuum pump and a liquid nitrogen vapor trap. The solvent was then introduced to the calorimeter cell at a steady flow rate of 3.3 ml/h by means of a syringe micropump, and two Valco Instrument changeover valves for switching between solvent and solution. The heat effect was recorded by



means of a strip chart recorder and a PC. After the thermal equilibrium was reached, which usually took 8 to 30 minutes, the solvent was switched over to the solvent containing adsorbate and the solution was introduced to the cell at a flow rate of 3.3 ml/h. The heat of interaction of adsorbate on the solid was also recorded using the strip chart recorder and PC. The recorded experimental data was analyzed using the Microscal Calorimeter Digital Output-Processing System (CALDOS). This program enables the analysis of the calibration and experimental data and converts the raw downloaded data into the heat of immersion ( $h_i$ ) and heat of adsorption ( $h_{ads}$ ) values.

#### 4.2.2.1 Heat of Adsorption of Butanol on Talc Surface from n-Heptane

The Microscal flow microcalorimeter was used to measure the heat of butanol adsorption on the powdered talc samples. The method of Groszek and Partyka (16) was used for determining the proportion of the hydrophilic sites on talc surfaces as described in Chapter 4.1.1. In these measurements, a talc sample was first equilibrated with n-heptane to establish a baseline on the chart recorder and PC. A butanol-in-heptane solution (2 g/l) was then introduced, and the heat effect recorded.

In the present work, a series of tests were also conducted to determine the heat of butanol adsorption from water (10 g/l) on talc using the flow microcalorimeter. However, no measurable quantity of heat of butanol adsorption on talc from water was observed. Probably, smaller butanol molecules were not able to displace the larger water molecules from the talc surface.

#### 4.2.2.2 Heat of Adsorption of Organic Acids and Bases on Talc Surface from Toluene

The percentages of acidic and basic sites on the surface of a talc sample were determined using the method described by Malhammar (19). In this method, the heats of adsorption of organic acids and bases on talc from toluene are measured using the flow microcalorimeter. The heats of adsorption results are then used to estimate the number of acidic and basic sites on the talc surface.

In these series of tests, a talc sample was first wetted with toluene and the heat effect due to immersional wetting was observed using the Microscal flow microcalorimeter. The flow of toluene was continued until a steady baseline was

established. The toluene flow was then replaced by a toluene solution containing 0.0125 moles/l of an organic acid (trifluoroacetic acid) or an organic base (butylamine). It was assumed that practically all of the acidic and basic sites reacted at 0.0125 M solution. A heat effect was observed when either the organic acid or base adsorbed on the talc surface.

The heat effect, which is due to the adsorption of the organic acid or base, is proportional to number of the basic and acidic sites of talc, respectively. In the present work, the percentage of the heats of adsorption of the organic acid and base were considered to be equal to the percentage of basic and acidic sites on talc surfaces, respectively.

#### 4.2.2.3 Determination of Areal Ratio Values of Talc Samples

The same procedure given in Chapter 4.2.2.1 was followed for determining the values of areal ratios (hydrophobic-to-hydrophilic surface area ratio) of various talc samples. The hydrophilic surface area of a talc sample was obtained from the heat of adsorption of butanol from n-heptane solution (2 g/l). The hydrophobic surface area of talc was calculated by subtracting the hydrophilic surface area from the total surface area. The areal ratios of talc samples were determined using Eq. [4.1].

#### 4.2.2.4 Determination of Surface Free Energy Components at the Basal and Edge Surfaces of Talc

The estimation of the surface free energies of basal and edge surfaces requires the knowledge of the fraction of the basal surface ( $f_b$ ) and that of the edge surface ( $f_e$ ) at two different size fractions, along with the surface free energy components of the two size fractions.

In the present work, a talc ore from the Yellowstone deposit was used for surface free energy characterization of basal and edge surfaces. The talc ore was ground to the nominal mean particle size of 12.5  $\mu\text{m}$  and 3.0  $\mu\text{m}$  using the same type of industrial scale mill at Luzenac America plants (25). These two talc samples are labeled as Yellowstone ( $d_{50}= 12.5 \mu\text{m}$ ) and Mistron Vapor-P ( $d_{50}=3.0 \mu\text{m}$ ), respectively. The fractions of basal

surface ( $f_b$ ) and edge surface ( $f_e$ ) of each talc sample were determined using the Groszek and Partyka method (20) as described in Chapters 4.1.1 and 4.2.2.1.

The surface free energy parameters of these two talc samples were estimated using Eq. [2.8]. In using Eq. [2.8], the contact angle values of various liquids on talc samples were obtained from the thin layer wicking measurements. In these measurements, 1-bromonaphthalene, methylene iodide, water, formamide and ethylene glycol were utilized as the test liquids. The contact angles measured with 1-bromonaphthalene, water and formamide were used to calculate the values of the surface free energy parameters ( $\gamma_s^{LW}$ ,  $\gamma_s^+$ , and  $\gamma_s^-$ ) of the talc samples. The details of measuring contact angles using the thin layer wicking technique are given in Chapter 2. It was observed that the contact angle results obtained from the thin layer wicking technique are more reliable than those determined using other techniques. Therefore, these results were chosen for the estimation of the surface free energy components at the basal and edge surfaces of talc.

### 4.3. RESULTS AND DISCUSSION

The experimental results obtained from flow microcalorimetric measurements were used to estimate the percentage of hydrophilic-hydrophobic and acidic-basic surface sites on various powdered talc surfaces. The flow microcalorimetry data was also used for the determination of basal to edge surface area ratio values of talc samples and surface free energies at the basal and edge surfaces of talc.

A typical thermogram including immersionsal wetting, electrical calibration and adsorption exotherms recorded by the FMC system is shown in Figure 4.3. This particular experimental output is for the adsorption of butanol in n-heptane on a Yellowstone talc sample.

#### 4.3.1. Percent Hydrophilic Surface

Table 4.1 shows the values of the heats of adsorption ( $-\Delta H_{ads}$ ) of butanol on various talc samples from n-heptane. The values are given in units of  $\text{mJ/m}^2$ . Also shown at the bottom of the table is the heat of adsorption of butanol on silica ( $197 \text{ mJ/m}^2$ ), as reported by Malandrini, et al (20). Knowing that silica is 100% hydrophilic,

which is responsible for the high heat of adsorption, one can normalize the value of  $-\Delta H_{\text{ads}}$  for talc with respect to that for silica. The values obtained in this manner should give the percentage hydrophilic surface of talc. Table 4.1 lists the values of percent hydrophilic surface and the total and specific hydrophilic surface area, along with the average particle size of each talc powder.

As shown in Table 4.1, the hydrophilic surface percentage of talc samples varies from 12.5% to 63.4%. The results show that the most hydrophobic talc is Select-A-Sorb (12.5% hydrophilic surface), while the most hydrophilic talc is Montana-ROM (63.4% hydrophilic). Note also that the talc powders with smaller particle size (e.g., Mistron Vapor-P, Mistron-100, Select-A-Sorb) show higher surface hydrophobicity, i.e., lower percentage of hydrophilic surface, compared to those of larger particle size (e.g., Montana-ROM, Vermont-ROM, Yellowstone). These findings are consistent with the contact angle measurement results as reported in Chapter 2.

A set of heat of butanol adsorption measurements have been performed on the Montana talc sample to further demonstrate the effect of particle size on the hydrophilic surface percentages of talc. In these experiments, the run-of-mine Montana talc sample was ground to below 212  $\mu\text{m}$  using an agate mortar and pestle, and then wet-screened into the 212 x 150, 150 x 75, 75 x 53 and 53 x 0  $\mu\text{m}$  size fractions. The heat of butanol adsorption on each size fraction from n-heptane was determined using the flow microcalorimeter. The results are given in Table 4.2. Figure 4.4 shows the heat of butanol adsorption on different particle size fractions from n-heptane, plotted as a function of average particle size,  $d_{50}$ .

It can be seen from Table 4.2 that the heat of butanol adsorption, and hence the percentage of hydrophilic surface, decreases with decreasing particle size, suggesting an increase in the surface hydrophobicity. As shown, 96.4% of the surface is hydrophilic at the 212 x 150  $\mu\text{m}$  size fraction, while 42.4% of the surface is hydrophilic at the 53  $\mu\text{m}$  x 0 size fraction. It is interesting to note that at very large particle size fractions, e.g. 212 x 150  $\mu\text{m}$ , the surface hydrophilicity of talc is comparable to the surface of silica. The results given in Table 4.2 suggest that the talc particles must be ground to below 53  $\mu\text{m}$  to produce highly hydrophobic surfaces. It is expected that the surface hydrophobicity of Montana talc would further increase by grinding it to smaller particle size.

#### 4.3.2. Acidic and Basic Site Distribution of Talc

The values of heats of adsorption of trifluoroacetic acid (TFAA) and butylamine (BA) on talc samples from toluene are reported in Table 4.3. Also shown in this table are the percentages of acidic and basic surface for the talc samples, estimated from the values of heats of trifluoroacetic acid and butylamine adsorption. Generally, the heats of adsorption were larger with TFAA than with BA, indicating that all the talc samples tested in the present work are basic.

It can be seen from Table 4.3 that Select-A-Sorb powder is the most basic surface with 90.3% basicity, while the Mistron-100 is the least basic surface with 56.8% basicity. Also shown, Mistron Vapor-P and Yellowstone talc samples also have significantly higher percentages of basic surface. The surface free energy parameters obtained from contact angle measurements also showed that the talc samples are mostly basic (see Chapter 2 and 3). Thus, the results, based on heat of adsorption measurements are in line with the results obtained from contact angle measurements. Furthermore, the basic surface property of talc reported here is also in good agreement with those reported by Wu et al (26).

The results given in Table 4.3 clearly indicate that the acid-base interactions play an important role in terms of the adhesion strength. As shown, the heat of interaction between talc and acidic adsorbate (TFAA) increases as the surface becomes more basic. For example, the highest heat of adsorption value of TFAA was obtained with Select-A-Sorb talc, while the lowest value was observed with Mistron-100 talc. On the other hand, the heat of butylamine adsorption on Select-A-Sorb talc was the lowest, suggesting that a basic reagent does not interact with a basic surface. The trend of heat of interaction reported here is in good agreement with those reported by Malhammar (19), who determined the surface basicity of talc from the heat of adsorption measurements using organic acids and bases as the probe liquids. The results presented here also confirm the validity and importance of acid-base interactions between two interacting surfaces as proposed by Fowkes (8, 27-28), van Oss et al. (29-34) and Berg (23). Since the talc surface is composed predominantly of basic surface sites, it would be an excellent adsorbent for acidic substances.

### 4.3.3. Areal Ratios of Talc Samples

A series of microcalorimetric measurements have been conducted on the Montana talc sample that was screened into various size fractions (212 x 150, 150 x 75, 75 x 53 and 53 x 0  $\mu\text{m}$ ) to show the effect of particle size on the values of basal-to-edge surface area ratios (areal ratio). The details of experimental procedure are given in Chapter 4.3.1. The values of areal ratios calculated using Eq. [4.1] for each size fraction are given in Table 4.4.

It can be seen from Table 4.4 that the values of areal ratios increase with decreasing particle size which is associated with an increase in the basal surface area. As shown, at 212 x 150  $\mu\text{m}$  size fraction the value of areal ratio is 0.04, while it increases to a value of 1.36 at 53  $\mu\text{m}$  x 0 size fraction. These results indicate that the basal (hydrophobic) to edge (hydrophilic) surface area ratio increases with decreasing particle size. Since there was not sufficient data regarding the contact angle values and, hence, surface free energy components at each size fraction, the surface free energies of basal and edge surfaces of Montana talc could not be determined. However, the contact angle, surface free energy components, and basal and edge surface areas of Yellowstone talc at two different sizes (i.e.,  $d_{50}=12.5 \mu\text{m}$  and  $3.0 \mu\text{m}$ ) were available, allowing us to determine the surface free energy parameters at the basal and edge surfaces of this talc.

Table 4.5 shows the values of basal to edge surface area ratios obtained for various powdered talc samples using the flow microcalorimeter. The values of the average size,  $d_{50}$ , and the total, hydrophobic and hydrophilic surface area for each talc sample are also listed in this table. The values of areal ratios for each talc sample were calculated using Eq. [4.1].

As can be seen in Table 4.5, Select-A-Sorb had the highest basal-to-edge surface area ratio among the talc samples studied, 6.97, followed by Mistron Vapor-P, 1.72, as expected. The microcalorimetric measurement results given in this chapter (see Table 4.1) and the contact angle and microcalorimetric measurement results presented in Chapters 2 and 3 showed that these are the two most hydrophobic surfaces; hence, the ratio between basal and edge surfaces should be the highest. On the other hand, the difference in the values of the areal ratios between Select-A-Sorb and Mistron Vapor-P is

considerably high. As shown in Table 4.4, the values of  $d_{50}$  for both Select-A-Sorb and Mistrion Vapor-P samples are also very close. Such a large difference between two areal ratio values may be attributed to the fact that the two talc are from two different mines and were produced using different processes.

The results presented in Table 4.5 shows that there is a correlation between the average particle size and the values of areal ratios. For example, the Montana talc, which has the highest value of  $d_{50}$  (63  $\mu\text{m}$ ), has the lowest value of areal ratio, 0.58. As shown, the areal ratios of talc particles increase gradually with decreasing particle size.

Also shown in Table 4.5 are the values of aspect ratios (dimensional) for Yellowstone and Mistrion Vapor-P talc samples as reported by the manufacturer (Luzenac America). These values were 0.9 and 1.4 for Yellowstone and Mistrion Vapor-P samples, respectively. In Luzenac America laboratories, the values of aspect ratios are determined using the particle size measurement and spectroscopic techniques in combination (25). In the present work, the values of areal ratios for Yellowstone and Mistrion Vapor-P obtained from microcalorimetric measurements were 1.19 and 1.72, respectively. Although one of the techniques gives dimensional aspect ratios and the other gives areal ratios; there is a good agreement between the dimensional aspect ratios determined using particle size measurements and spectroscopic techniques in combination, and the areal aspect ratios determined using microcalorimetric measurements. Obviously, by studying a large number of talc samples, a better correlation between the areal and dimensional aspect ratios could be obtained.

As can be seen in Table 4.5, the average particle size for Yellowstone and Mistrion Vapor-P samples were 12.5  $\mu\text{m}$  and 3.0  $\mu\text{m}$ , respectively. On the other hand, the values of both dimensional and areal aspect ratios are higher for Mistrion Vapor-P compared to that of Yellowstone talc. As discussed before, these two samples were produced from the head Yellowstone ore by grinding it in the same type of mill as used in the plant. Thus, the data presented here reveals one more time that the more hydrophobic basal surfaces are created by grinding and therefore, the value of basal-to-edge-surface area ratio increases as the particles become finer.

One of the most important advantages of using microcalorimetry technique for determining the areal aspect ratios of solid surfaces over other techniques is that it is fast,

simple, and more reliable. It gives the areal aspect ratio values of bulk particles, rather than a single particle or few particles. The evaluation of results is objective, unlike the TEM or SEM measurements.

#### 4.3.4. Surface Free Energies of Talc at Basal and Edge Surfaces

The results presented in the previous sections suggest that the surface hydrophobicity and areal ratios of talc particles increase with decreasing particle size. However, these results do not explain important subjects such as: 1) the surface free energies at the basal and edge surfaces of talc, 2) the number of acidic and basic sites available at the basal and edge surfaces. The answers to these important questions are required for a complete explanation of the surface properties of talc. The main objective of the present work was, therefore, to find out the answers of these questions.

The principal idea of this work is summarized in Table 4.9. However, in order to estimate the surface free energies of basal and edge surfaces, it was necessary to know the fraction of the basal surface ( $f_b$ ) and that of the edge surface ( $f_e$ ) at two different size fractions and also the surface free energy components of these two size fractions.

The fractions of basal and edge surfaces for Yellowstone ( $d_{50}=12.5 \mu\text{m}$ ) and Mistron Vapor-P ( $d_{50}=3.0 \mu\text{m}$ ) samples were obtained from microcalorimetric measurements. The results are presented in Table 4.6. As shown, the value of  $f_b$  is higher for the finer Mistron Vapor-P talc sample (0.632) than the coarser Yellowstone talc sample (0.543). Also shown are  $f_b$  and  $f_e$  values of Yellowstone and Mistron Vapor-P powders reported by the manufacturer. Although there is a small difference between the values obtained in the present work and those reported by the manufacturer, the trend is similar. The finer Mistron Vapor-P talc sample has a higher value of  $f_b$  compared to those of the coarser Yellowstone talc.

Table 4.7 gives the advancing contact angle values of various liquids on Yellowstone and Mistron Vapor-P samples obtained from thin layer wicking measurements. As shown, the contact angles on the Mistron Vapor-P talc were higher than those obtained on the Yellowstone talc, regardless of the liquid chosen. For example, the measured water contact angle on the Yellowstone surface was  $84.5^\circ$ , while it increased to  $85.5^\circ$  on the Mistron Vapor-P surface. The highest increments in the



values of contact angles from the Yellowstone surface to the Mistron Vapor-P surface were obtained with formamide and ethylene glycol, two basic liquids.

The values of contact angles given in Table 4.7 for the thin layer wicking technique were used to calculate the Lifshitz-van der Waals ( $\gamma_s^{LW}$ ), Lewis electron donor ( $\gamma_s^-$ ) and electron acceptor ( $\gamma_s^+$ ) components of the surface free energy on the Yellowstone and Mistron Vapor-P talc samples using Eq. [4.2]. As discussed in previous chapters, the calculation requires a set of three contact angles for three different liquids, along with their surface tension components. The values of  $\gamma_L^{LW}$ ,  $\gamma_L^+$ , and  $\gamma_L^-$  for liquids were taken from literature (See Table 2.1). For a given talc surface, the contact angles measured using three test liquids -1-bromonaphthalene, water and formamide- were used for calculating the surface free energy components of talc samples. The results are shown in Table 4.8. Also shown in this table are the values of  $\gamma_s^{AB}$  ( $=2\sqrt{\gamma_s^+\gamma_s^-}$ ) and  $\gamma_s$  calculated using Eq. [4.3] from the values of the surface free energy components.

It can be seen from Table 4.8 that the values of both the  $\gamma_s^{LW}$  and  $\gamma_s^{AB}$  components on the Yellowstone talc surface are higher than those obtained on the Mistron Vapor-P surface. As shown, the  $\gamma_s^{LW}$  for the Yellowstone talc was 23.3 mJ/m<sup>2</sup>, while it decreased to 20.6 mJ/m<sup>2</sup> on the Mistron Vapor-P surface. Similarly, the value of  $\gamma_s^{AB}$  decreased from 5.1 mJ/m<sup>2</sup> on the Yellowstone talc surface to 4.8 mJ/m<sup>2</sup> on the Mistron Vapor-P surface.

Also shown in Table 4.8 are the values of  $\gamma_s^-$  and  $\gamma_s^+$ . As shown, the  $\gamma_s^-$  component on the Mistron Vapor-P surface is higher compared to those obtained on the Yellowstone talc. The opposite is true for the  $\gamma_s^+$  component. The  $\gamma_s^+$  on the Yellowstone talc surface is slightly higher than the Mistron Vapor-P surface. The value of  $\gamma_s^-$  is, however, much higher both on the Yellowstone and Mistron Vapor-P talc surfaces compared to the value of  $\gamma_s^+$ .

Also shown in Table 4.8, the total surface free energy ( $\gamma_s$ ) of the Yellowstone talc was 28.4 mJ/m<sup>2</sup>, but decreased to 25.4 mJ/m<sup>2</sup> on the Mistron Vapor-P talc. However, the decrease in the value of  $\gamma_s$  is associated with decreases in the values of both the  $\gamma_s^{LW}$  and  $\gamma_s^{AB}$  components. As the Mistron Vapor-P talc was found to be more hydrophobic from the contact angle measurements, it was expected the value of  $\gamma_s$  of the Mistron Vapor-P

talc should be lower than that of the Yellowstone talc. Thus, the data presented in this table reflects the results of contact angle measurements. The results presented in Table 4.8 also suggest that the values of  $\gamma_s$ ,  $\gamma_s^{LW}$  and  $\gamma_s^{AB}$  decrease with decreasing particle size.

Table 4.9 shows the values of surface free energy ( $\gamma_s$ ) and its components ( $\gamma_s^{LW}$ ,  $\gamma_s^-$ ,  $\gamma_s^+$  and  $\gamma_s^{AB}$ ) for the basal and edge surfaces of talc obtained using two different techniques. Based on the values of basal fraction ( $f_b$ ) and edge fraction ( $f_e$ ) and the surface free energy components obtained for two sizes ( $d_{50}=12.5 \mu\text{m}$  and  $3.0 \mu\text{m}$ , respectively), Eqs. [4.2] and [4.3] were solved simultaneously to calculate the values of relevant surface free energy parameters at the basal and edge surfaces. The values of  $f_b$  and  $f_e$  obtained from two different measurement techniques, i.e., microcalorimetric and particle size and spectroscopic measurements, are given in Table 4.6. The values of surface free energy parameters obtained from contact angle measurements at two size fractions are shown in Table 4.8. As can be seen in Table 4.9, the surface free energy parameters of the basal and edge surfaces determined using two different techniques are in good agreement.

The results given in Table 4.9 shows some very important trends that are need to be discussed. *First of all*, the surface free energy,  $\gamma_s$ , at the basal surface of talc is much smaller than that obtained at the edge surface. As shown, the value of  $\gamma_s$  at the basal surface obtained from microcalorimetric measurements is  $13 \text{ mJ/m}^2$ , whereas it is  $46.7 \text{ mJ/m}^2$  at the edge surface. The results reported here are in excellent agreement with those reported by Yariv (1), who determined the hydrophobicity of basal surfaces and relatively lower hydrophobicity of edge surfaces from contact angle measurements. By preparing the cleaved talc surfaces in various directions, Yariv (1) experimentally showed that the basal surfaces of talc have a water contact angle value of  $83^\circ$ , while the edge surfaces have a contact angle value of  $62^\circ$ . It also needs to be pointed out that the  $\gamma_s$  values reported in the literature for various hydrophobic polymer surfaces range from  $10.4\text{-}25.5 \text{ mJ/m}^2$  (35, 36). Thus, the value of  $\gamma_s=13 \text{ mJ/m}^2$  obtained for the basal surface suggests that the basal surface of talc may be categorized as a polymeric surface.

Furthermore, the value of  $46.7 \text{ mJ/m}^2$  obtained for the edge surface of talc seems to be a characteristic number for a hydrophobic surface whose advancing water contact angle ( $\theta_a$ ) is  $62^\circ$ . Pazhianur (37) determined the surface free energy parameters of

silanated silica surfaces with varying hydrophobicities from contact angle measurements. This author reported the  $\gamma_s$  values for silanated silica surfaces exhibiting  $\theta_a=50^\circ$  and  $75^\circ$  were  $52.8 \text{ mJ/m}^2$  and  $42.6 \text{ mJ/m}^2$ , respectively. From these results, by extrapolation, a value of  $47.6 \text{ mJ/m}^2$  for  $\gamma_s$  can be obtained at  $\theta_a=62^\circ$ . Wu et al (26) showed that the value of  $\gamma_s$  on the powdered silica surface was  $48.7 \text{ mJ/m}^2$  at  $\theta_a=58.9^\circ$ . In the present work, from the contact angle measurements conducted on the flat Vermont talc surface, it has also been determined that the value of  $\gamma_s$  for the talc surface is  $48.0 \text{ mJ/m}^2$  at  $\theta_a=62.3^\circ$  (See Table 2.10). Hence, the value of  $\gamma_s$  reported here for the edge surfaces agrees well what has been published in the literature.

*Second*, similar to the values of  $\gamma_s$ , the  $\gamma_s^{\text{LW}}$  component at the basal surface of talc is much smaller than that obtained at the edge surface. According to Table 4.9, the  $\gamma_s^{\text{LW}}$  value, obtained from microcalorimetric measurements, at the basal surface is  $9.4 \text{ mJ/m}^2$ , while it is  $39.8 \text{ mJ/m}^2$  at the edge surface. Table 4.9 also shows that the  $\gamma_s^{\text{LW}}$  value obtained from particle size measurements at the basal surface is slightly higher than ( $10.3 \text{ mJ/m}^2$ ) those obtained from microcalorimetric measurements ( $9.4 \text{ mJ/m}^2$ ). It should be noted that the values reported in the literature for hydrophobic polymer surfaces range from  $10.4\text{-}25.5 \text{ mJ/m}^2$  (35, 36). The values of both  $\gamma_s^{\text{LW}}$  and  $\gamma_s$  were essentially the same for the hydrophobic polymer surfaces, since the surface of these polymers consists only of the Lifshitz-van der Waals free energy component. Thus, the value of  $\gamma_s^{\text{LW}}$  reported here is very close to the values reported by Fowkes (35) for the deposited films of  $\phi$ -dodecanoic acid on the Pt surface.

*Third*, the value of  $\gamma_s^-$  is much higher than the value of  $\gamma_s^+$  for the basal surfaces of talc. The results indeed did show that the  $\gamma_s^+$  component at the basal surface has a negative value, obtained with either of the techniques used. On the contrary, the  $\gamma_s^+$  component is higher than the  $\gamma_s^-$  component at the edge surface of talc. Interestingly, the  $\gamma_s^-$  component exhibited a negative value in the case of the edge surface. The negative values reported here explain that some more corrections are still needed to determine the values of  $f_b$  and  $f_e$ . The negative values given in Table 4.9, however, can be assumed to be zero. Nevertheless, these results suggest that both the basal surface and edge surface of talc are monofunctional, i.e., the basal surface is *basic* and the edge surface is *acidic*.

It should be noted that these are only the preliminary results and are part of an ongoing project. Determination of the surface free energies of the basal and edge surfaces of talc samples from different origins (i.e., macrocrystalline and microcrystalline talc) using different particle size fractions would be a very interesting future work.

From the results presented in Table 4.9, it becomes clear now why the basal surfaces of talc are basic and the edge surfaces are acidic. Recall that the basal planes of talc are made up of fully compensated oxygen atoms, linked together by siloxane (Si-O-Si) bonds, and the edges are composed of MgOH, SiOH and the other substituted cations, e.g. Al<sup>3+</sup>, Fe<sup>2+</sup> (1-5). Hence, the basic nature of the basal plane surface of talc reported here should be attributed to the basic oxygen atoms oriented at the basal planes, while the acidic character of the edge surfaces should be attributed to the surface silanol groups (SiOH) and other substituted cations which tend to accept electrons during acid-base interactions.

Finally, the basal and edge surfaces of talc both have the  $\gamma_s^{AB}$  component, although the value of  $\gamma_s^{AB}$  on the basal surface is smaller compared to that obtained at the edge surface. According to Table 4.9, the  $\gamma_s^{AB}$  value at the basal surface is 3.6 mJ/m<sup>2</sup>, whereas it is 6.9 mJ/m<sup>2</sup> at the edge surface. It is interesting to note that the contribution of the  $\gamma_s^{AB}$  component to the surface free energy of the basal surface of talc is surprisingly high. This seems to be in contrast to the definition of  $\gamma_s^{AB}$  made by Van Oss-Chaudhury-Good (26, 32-34). This is an important point that needs to be made clear here. According to Eq. [4.3], the  $\gamma_s^{AB}$  is given by

$$\gamma_s^{AB} = 2\sqrt{\gamma_s^+ \gamma_s^-} \quad [4.6]$$

so that  $\gamma_s^{AB}$  will take zero values for three conditions: i) when  $\gamma_s^- = 0$  and  $\gamma_s^+ \neq 0$ , ii) when  $\gamma_s^- \neq 0$  and  $\gamma_s^+ = 0$ , or iii) when  $\gamma_s^- = \gamma_s^+ = 0$ . It has already been discussed that the basal and edge surfaces of talc are both monofunctional, that the basal surface is basic and the edge surface is acidic. This means that one of the parameters in the right hand side of Eq. [4.6] will take a zero value and so does the  $\gamma_s^{AB}$ . However, the results given in Table 4.9 suggest that  $\gamma_s^{AB}$  doesn't take a zero value, although either  $\gamma_s^-$  or  $\gamma_s^+$  is zero on the basal

or edge surfaces of talc. Even for such a hydrophobic solid surface (the basal surface of talc), the contribution of  $\gamma_s^{AB}$  to the surface free energy is considerably high. Probably, a zero value for  $\gamma_s^{AB}$  on a solid surface is attained only in the case of condition (iii), i.e., when both  $\gamma_s^-$  and  $\gamma_s^+$  are zero.

#### 4.4. CONCLUSIONS

Heats of adsorption measurements were conducted to determine the values of basal-to-edge surface ratios of talc particles and the surface free energy components at the basal and edge surfaces of the talc mineral. The surface free energy components ( $\gamma_s^+$ ,  $\gamma_s^-$ ,  $\gamma_s^{AB}$  and  $\gamma_s^{LW}$ ) at the basal and edge surfaces of talc were obtained using the Van Oss, Chaudhury and Good (VCG) thermodynamic approach.

The results showed that the basal surfaces of talc contains only the basic component of surface free energy ( $\gamma_s^-$ ), suggesting the mono-functionality of basal surfaces of talc, e.g. basic. Interestingly, the edge surfaces contains only acidic component ( $\gamma_s^+$ ), which also suggest the mono-functionality of edge surfaces, e.g. acidic. The results also showed that the surface free energy ( $\gamma_s$ ) at the basal surface is substantially smaller compared to that obtained at the edge surface.

The results from microcalorimetric studies indicated that the acid-base interactions play an important role between two interacting surfaces. The results showed that the heat of adsorption enthalpies of organic acids increased substantially with increasing surface basicity of the talc samples. The heat of adsorption data showed that the number of basic sites for all talc samples studied is higher than the number of acidic sites. The surface free energy data also showed that overall the surface of talc is basic, which suggests that talc can serve as an excellent adsorbent for acidic adsorbates. By the same token, the talc samples characterized in the present work may serve as ideal fillers for acidic matrices.

The results showed that there is a relationship between particle size and the basal-to-edge surface area ratios, and as the particle size decreases the areal ratio increases. This can be attributed due to the fact that more nonpolar basal plane surfaces are created

and hence, the ratio between the basal to edge area increases when the particles become finer.

A linkage between particle hydrophobicity and surface free energy components was also established. As a general trend, the  $\gamma_s^{AB}$  and  $\gamma_s^{LW}$  components of surface free energy decrease with decreasing particle size, and so does the value of  $\gamma_s$ . The more the surface is hydrophobic, the lower the  $\gamma_s$  is. However, this is associated with decreases both in the values of both  $\gamma_s^{LW}$  and  $\gamma_s^{AB}$ .

#### 4.5. REFERENCES

1. Yariv, S., *Wettability of Clay Minerals*, in: *Modern Approaches to Wettability: Theory and Applications*, Eds: M. E. Schrader, and G. Loeb, Plenum Press, New York, pp. 279-326, 1992.
2. Chander, S., Wie, J. M. and Fuerstenau, D. W., in: *Advances in Interfacial Phenomena*, Ed: P. Somasundaran, AIChE Series No. 150, New York, pp.183-188, 1975.
3. Fuerstenau, M. C., Lopez-Valdiviezo, A., and Fuerstenau, D.W., *Int. J. of Mineral Proc.*, 23, 161-170, 1988.
4. Ciullo, P. A., in: *Industrial Minerals and Their Uses-A Handbook and Formulary*, Ed: P. A. Cuillo, Noyes Publications, New Jersey, 1996.
5. Rayner, J. H., and Brown, G., *Clays and Clay Minerals*, Vol. 21, 103-114, 1973.
6. Fourchet, G., *Polymer Eng. Sci.*, 35, 957, 1995.
7. Pukansky, B., in: *Polypropylene: Structure, Blends and Composites*, Ed: J. Karger-Kocsis, Vol. 3, pp. 1, Chapman and Hall, London, 1995.
8. Fowkes, F.M., in: *Physicochemical Aspects of Polymer Surfaces*, Ed: K.L. Mittal, vol. 2, p. 583, Plenum Press, New York, 1983.
9. Schlumpf, H. P., *Synthetic* 12,31, 1981.
10. Nakatsuka, T., *Polym. Sci. Technol.* 27, 51, 1985.
11. Groszek, A. J., *Nature*, 196, 531, 1962.
12. Groszek, A. J., *Proc. Roy. Soc., A*, 314, pp. 473-498, 1970.
13. Groszek, A. J., *Chemistry and Industry*, October 15, pp. 1754-1756, 1966.

14. Templer, C. E., *Nature Physical Science*, Vol. 235, No. 60, February 21, pp. 158-160, 1972.
15. Groszek, A. J., *Carbon*, Vol. 25, No.6, pp. 717-722, 1987.
16. Groszek, A. J., and Partyka, S., *Langmuir*, 9, pp. 2721-2725, 1993.
17. Basilio, C., *Ph.D. Thesis*, Virginia Tech, 1989.
18. Fowkes, F. M., and Joslin, S. T., *in Ref. 6*, 1983.
19. Malhammar, G., *Colloids and Surfaces*, 44, pp. 61-69, 1990.
20. Malandrini, H., Clauss, F., Partyka, S., and Douillard, J. M., *J. Colloid and Interface Sci.*, 194, 183-193, 1997.
21. Fowkes, F. M., *Polym. Mater. Sci. Engr.*, 51, pp. 522-527, 1984.
22. Fowkes, F. M., Tishler, D. O., Wolfe, J. A., Lannigan, L. A., Ademu-John, C. M., and Halliwell, M. J., *J. Polym. Sci. Chem. Ed.*, 22, pp. 547-566, 1984.
23. Berg, J. C., *Nordic Pulp and Paper Research Journal*, 1, 75-85, 1993.
24. Lohmander, S., *Nordic Pulp and Paper Research Journal*, Vol. 15, No. 3, pp. 221-230, 2000.
25. Yordan, 2000. *Personal communication*
26. Wu, W., Griese, R.F. Jr., and van Oss C.J., *Powder Technology*, 89, 129-132, 1996.
27. Fowkes, F.M., and Mostafa, M.A., *Industrial and Engineering Chemistry Prod. Res. Dev.*, 17, 3, 1978.
28. Fowkes, F.M., in: *Surface and Interfacial Aspects of Biomedical Polymers*, Ed: J. D. Andrade, Plenum Press, New York, Vol. I, pp. 337-372, 1985.
29. Van Oss, C. J., Good, R. J., and Chaudhury, M. K., *J. of Colloid and Interface Science*, 111, 378, 1986.
30. Van Oss, C. J., Chaudhury, M. K., and Good, R. J., *J. Separation Sci. and Technology*, 22, 1, 1987.
31. Van Oss, C. J., Chaudhury, M. K., and Good, R. J., *J. of Colloid and Interface Science*, 128, 313, 1988.
32. Van Oss, C. J., Chaudhury, M. K., and Good, R. J., *Adv. Colloid Interface Science*, 28, pp. 35-64, 1987.
33. Van Oss, C. J., Chaudhury, M. K., and Good, R. J., *J. Colloid Interface Science*, 128, 313, 1989.

34. Good, R. J., and van Oss, C. J., in *Modern Approaches to Wettability: Theory and Applications*, Eds: M. E. Schrader, and G. Loeb, Plenum Press, New York, pp. 1-27, 1992.
35. Fowkes, F.M., *Industrial and Engineering Chemistry*, 56/12, 40, 1964.
36. Zisman, W. A., *Advan. Chem.*, 43, 1, 1964.
37. Pazhianur, R., *Ph.D. Thesis*, Virginia Tech, 1999.



Table 4.1. % Hydrophilic surface and specific hydrophilic surface area of the talc samples

Talc Sample	$-\Delta H_{ad}$ of Butanol on Talc from n-Heptane ( $\text{mJ}/\text{m}^2$ )	% Hydrophilic Surface	$d_{50}$ ( $\mu\text{m}$ )	Specific Surface ( $\text{m}^2/\text{g}$ )	
				Total <sup>(2)</sup>	Hydrophilic Surface
Montana -ROM	125.0	63.4	63.0	7.65	4.85
Vermont -ROM	89.5	45.4	$\approx 20.0$	2.6	1.20
Yellowstone	90.0	45.7	12.5	9.5	4.34
Mistron-100	84.5	42.9	3.5	13.0	5.58
Mistron Vapor-P	72.5	36.8	3.0	13.0	4.78
Select-A-Sorb	24.6	12.5	3.4	11.0	1.38
Silica (Reference)	197 <sup>(1)</sup>	100.0		--	--

<sup>(1)</sup> from Malandrini et al (1997)

<sup>(2)</sup> from BET measurements.

Table 4.2. Effect of particle size on the values of % hydrophilic surface and hydrophilic surface area for Montana talc

Particle Size ( $\mu\text{m}$ )	$-\Delta H_{ads}$ of Butanol on Talc from n-Heptane ( $\text{mJ}/\text{m}^2$ )	% Hydrophilic Surface	Specific Surface ( $\text{m}^2/\text{g}$ )	
			Total <sup>(2)</sup>	Hydrophilic Surface
212 x 150	190.0	96.4	6.1	5.88
150 x 75	152.0	77.2	6.9	5.32
75 x 53	125.0	63.4	7.65	4.85
53 x 0	83.6	42.4	11.1	4.71
Silica (Reference)	197 <sup>(1)</sup>	100.0	--	--

<sup>(1)</sup> from Malandrini et al (1997)

<sup>(2)</sup> from BET measurements

Table 4.3. Heat of displacement enthalpies of trifluoroacetic acid (TFAA) and butylamine (BA) from toluene on various talc powders

Talc Sample	- $\Delta H_{\text{disp}}$ on Talc from Toluene (mJ/m <sup>2</sup> )		% Surface Sites	
	TFAA	BA	Acidic	Basic
Vermont – ROM	261.7	150.4	36.5	63.5
Montana – ROM	116.8	84.1	41.9	58.1
Yellowstone	191.6	57.6	23.1	76.9
Mistron-100	152.3	115.6	43.8	56.8
Mistron Vapor-P	262.0	60.2	18.7	81.3
Select-A-Sorb	301.3	32.5	9.7	90.3

Table 4.4. Effect of particle size on the values of hydrophobic/hydrophilic surface sites and of basal-to-edge area ratios for Montana talc

Particle Size ( $\mu\text{m}$ )	Specific Surface (m <sup>2</sup> /g)			<i>Basal-to-Edge Area Ratio</i> <sup>(1)</sup>
	Total <sup>(2)</sup>	Hydrophilic Surface	Hydrophobic Surface	
212 x 150	6.1	5.88	0.22	0.04
150 x 75	6.9	5.32	1.58	0.30
75 x 53	7.65	4.85	2.80	0.58
53 x 0	11.1	4.71	6.39	1.36

<sup>(1)</sup> determined from Areal ratio = basal (hydrophobic) surface area / edge (hydrophilic) surface area

Table 4.5. Basal-to-edge ratio values of various talc samples determined using flow microcalorimeter

Talc Sample	Specific Surface (m <sup>2</sup> /g)		d <sub>50</sub> (μm)	<i>Basal-to-Edge Area Ratio</i> <sup>(1)</sup>	
	Total	Hydrophilic Surface			Hydrophobic Surface
Montana-ROM	7.65	4.85	2.80	63.0	0.58
Vermont-ROM	2.6	1.20	1.40	≈20.0	1.16
Yellowstone	9.5	4.34	5.16	12.5	1.19 <sup>(2)</sup>
Mistron-100	13.0	5.58	7.42	3.5	1.33
Mistron Vapor-P	13.0	4.78	8.22	3.0	1.72 <sup>(3)</sup>
Select-A-Sorb	11.0	1.38	9.62	3.4	6.97

<sup>(1)</sup> determined from *Areal ratio* = basal (hydrophobic) surface area / edge (hydrophilic) surface area

<sup>(2)</sup> the value of aspect ratio determined at Luzenac America is 0.9

<sup>(3)</sup> the value of aspect ratio determined at Luzenac America is 1.4.

Table 4.6. The fraction of the basal surface ( $f_b$ ) and that of the edge ( $f_e$ ) surface obtained from two different measurement techniques

Talc Sample	From Microcalorimetric Measurements		From Particle Size and Spectroscopic Measurements <sup>(1)</sup>	
	$f_b$	$f_e$	$f_b$	$f_e$
Yellowstone ( $d_{50}=12.5 \mu\text{m}$ )	0.543	0.457	0.4737	0.5263
Mistrion Vapor-P ( $d_{50}=3.0 \mu\text{m}$ )	0.632	0.368	0.5835	0.4165

<sup>(1)</sup> as determined in Luzenac America laboratories

Table 4.7. Contact angles (degree) of various liquids on Yellowstone and Mistrion Vapor-P talc samples measured using thin layer wicking technique (at  $20\pm 2 \text{ }^\circ\text{C}$ )

Talc Sample	1-Br	MI	W	FO	EG
Yellowstone ( $d_{50}=12.5 \mu\text{m}$ )	63.4 $\pm$ 1.8	72.2 $\pm$ 1.6	84.5 $\pm$ 2.0	67.2 $\pm$ 1.8	65.2 $\pm$ 1.8
Mistrion Vapor-P ( $d_{50}=3.0 \mu\text{m}$ )	68.7 $\pm$ 1.6	74.8 $\pm$ 1.5	85.5 $\pm$ 1.6	72.0 $\pm$ 1.5	71.5 $\pm$ 1.8

*1-Br=1-Bromonaphthalene, MI=Methylene iodide, W=Water, FO=Formamide, EG=Ethylene glycol*

Table 4.8. Surface Free energy components and parameters (mJ/m<sup>2</sup>) for Yellowstone and Mistron Vapor-P talc powders obtained from thin layer wicking measurements

	Yellowstone (d <sub>50</sub> =12.5 μm)	Mistron Vapor-P (d <sub>50</sub> =3.0 μm)
$\gamma_s^{LW}$	23.3	20.6
$\gamma_s^+$	1.1	0.8
$\gamma_s^-$	5.8	7.3
$\gamma_s^{AB}$	5.1	4.8
$\gamma_s$	28.4	25.4

Table 4.9. Surface free energy components and parameters (mJ/m<sup>2</sup>) at the basal and edge surfaces of talc obtained using two different basal-to-edge ratio determination techniques

	From Microcalorimetric Measurements		From Particle Size Measurements	
	Basal Surface	Edge Surface	Basal Surface	Edge Surface
$\gamma_s^{LW}$	9.4	39.8	10.3	35.9
$\gamma_s^{AB}$	3.6	6.9	3.7	6.5
$\gamma_s^-$	13.5	-3.3	13.0	-0.7
$\gamma_s^+$	-0.44	2.93	-0.34	2.4
$\gamma_s$	13.0	46.7	14.0	41.4

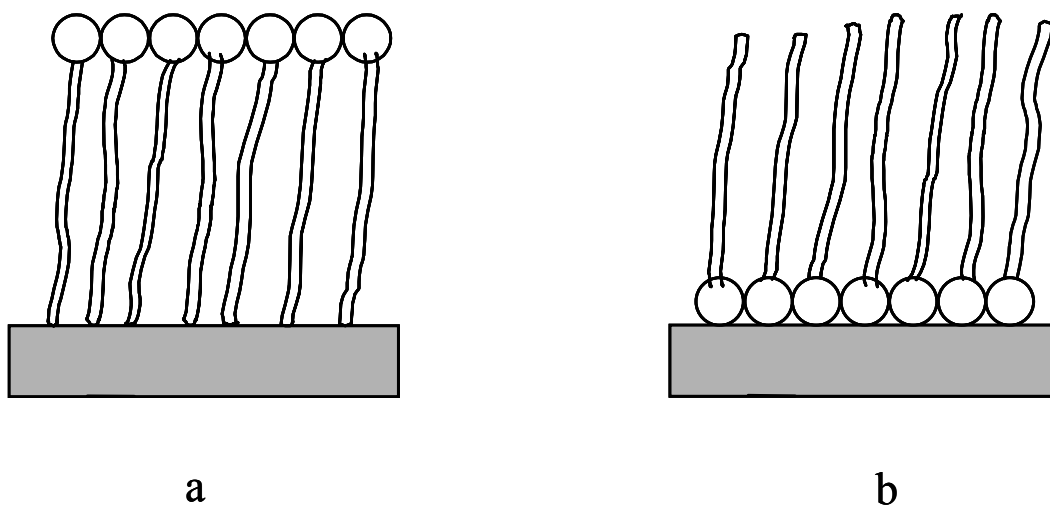


Figure 4.1. Schematic representation of (a) butanol adsorbed on talc from water (b) butanol adsorbed on talc from n-heptane.

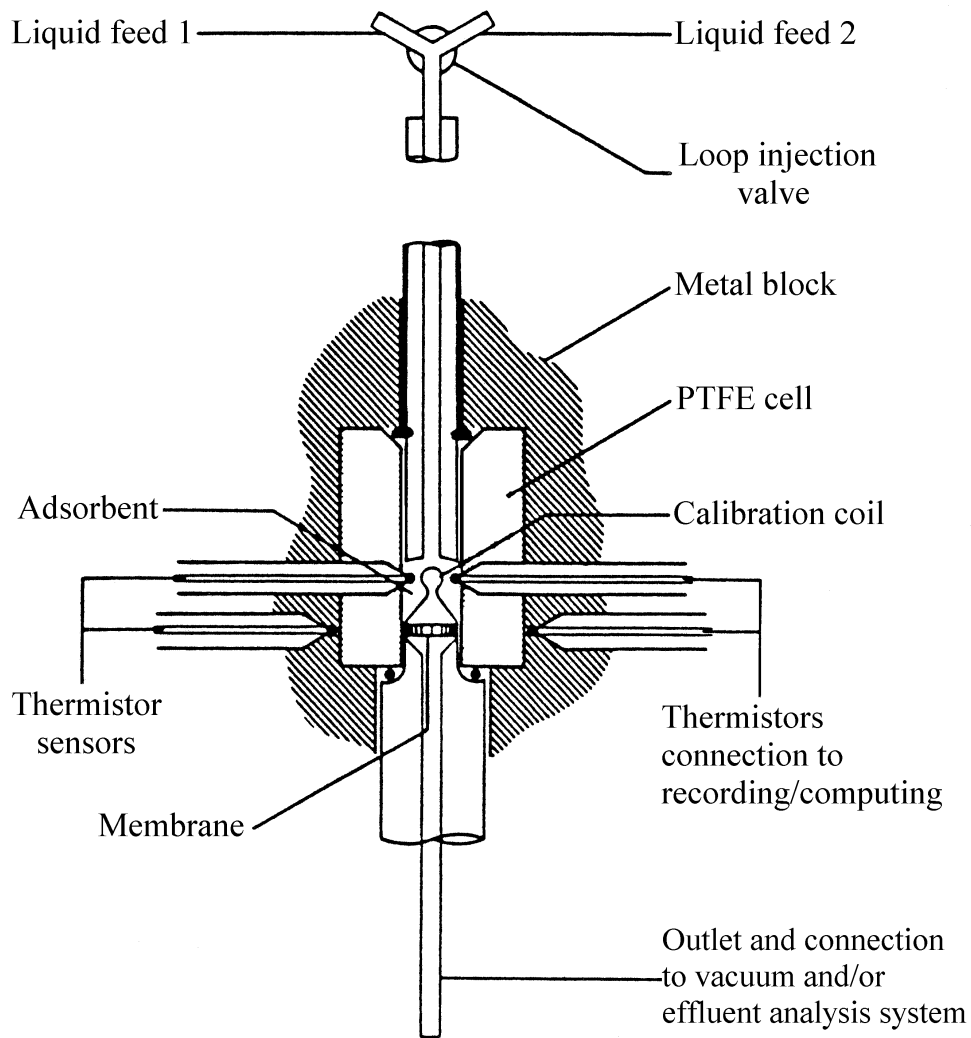


Figure 4.2. Schematic diagram of the flow microcalorimeter used for the adsorption and displacement studies

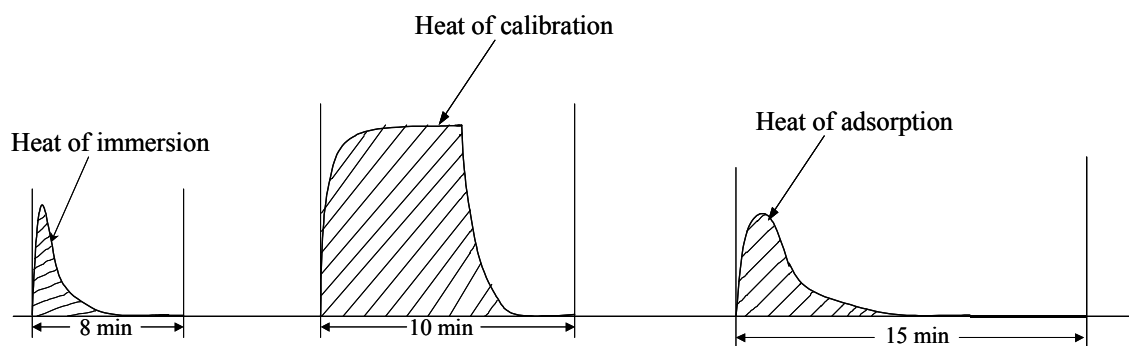


Figure 4.3. Typical thermal output of flow microcalorimeter including heat of immersion (n-heptane), heat of calibration, and heat of adsorption (butanol) peaks obtained for Yellowstone talc sample. Areas under the curves are proportional to the heat created.



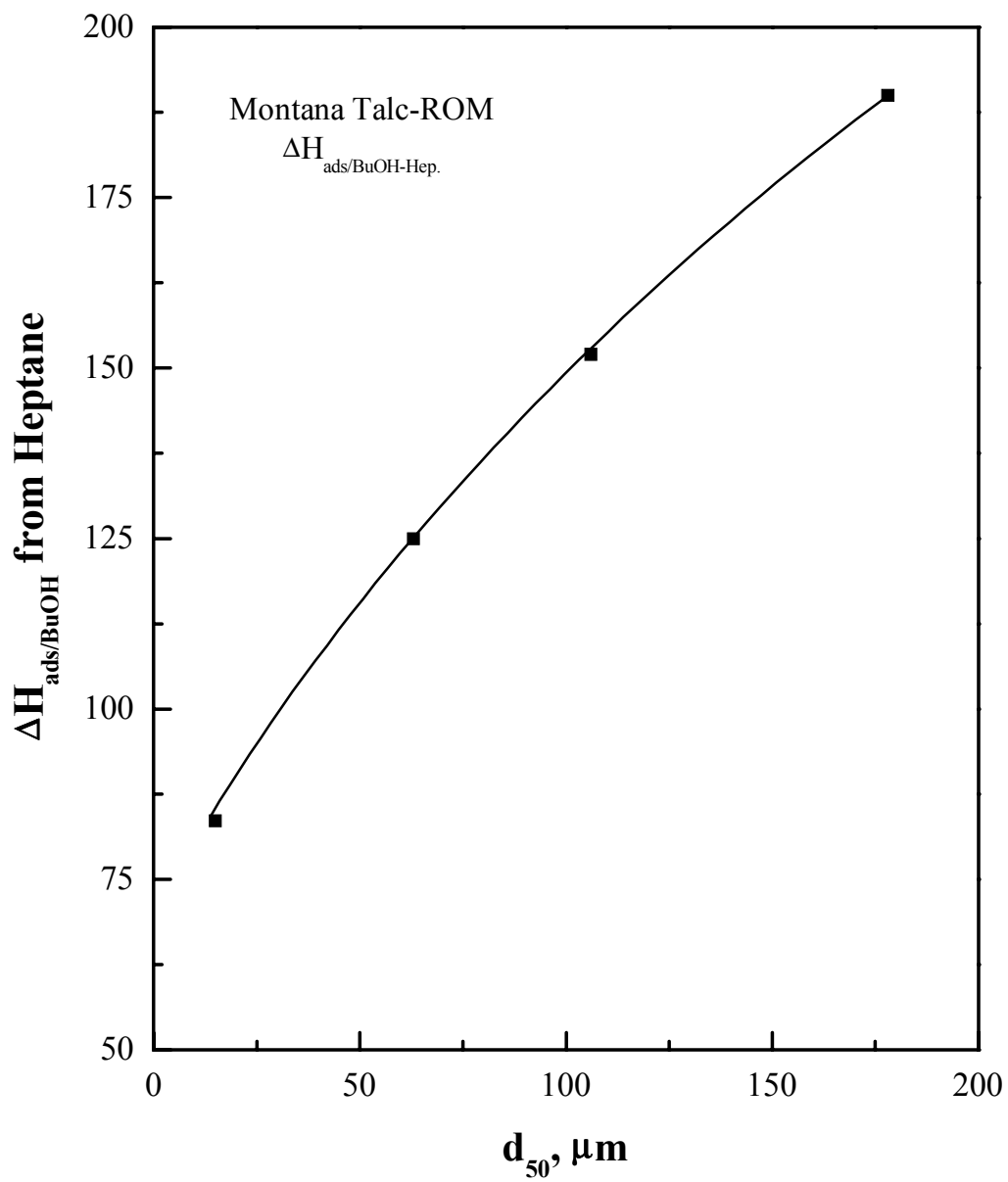


Figure 4.4. Change in the values of heat of adsorption enthalpies of butanol from n-heptane on the Montana talc surface as a function of particle size